Regulation of the orphan receptor Gpr176 activity via post-translational modifications in the central circadian clock

（概日時計中枢における翻訳後修飾を介したオーファン受容体 Gpr176 の活性調節）

２０２２

王　甜宇

CONTENTS

PREFACE

G-protein-coupled receptors (GPCRs) are important drug targets with diverse therapeutic applications. However, there are still more than a hundred orphan GPCRs, whose protein functions and biochemical features remain unidentified. Gpr176 is one of these so-called orphan GPCRs. *Gpr176* (also known as *HB-954*) was initially cloned from a human brain cDNA library by Hata *et al.* By generating and analysing *Gpr176*-deficient mice, a previous study in our laboratory revealed that in the mouse brain, *Gpr176* is most abundantly expressed in the suprachiasmatic nucleus (SCN), the locus of the principal circadian pacemaker in the brain and demonstrated that this GPCR is required for keeping the pace of normal circadian behavioural activity rhythm. Therefore, Gpr176 has been regarded as a promising therapeutic target for insomnia and lifestyle-related diseases. However, biochemical characteristics are largely unknown for Gpr176. In this study, I focused on characterising protein function and biochemical feature of Gpr176 and discovered that the level of cellular Gpr176 activity is regulated by *N*-glycosylation (**Chapter 1**) as well as by phosphorylation (**Chapter 2**).

Chapter 1: Identification and functional characterisation of *N*-linked glycosylation of the orphan G-protein-coupled receptor Gpr176.

N-glycosylation is one of the most common post-translational modifications for GPCRs. However, not surprisingly, knowledge regarding the presence and potential functional role of *N*-linked glycosylation for orphan GPCRs has been particularly sparse, compared to that of receptors with known ligands. Previous studies based on GPCRs with known ligands demonstrated that *N*-glycosylation may be important for their structural maturation, cell surface expression, ligand binding, and downstream signal transduction. However, the functional role(s) of *N*-glycosylation varied depending on the type of GPCRs tested. Because of this non-redundant functional nature of *N*-glycosylation, its role for Gpr176 must be determined empirically.

In this chapter, I first provide evidence that Gpr176 is *N*-glycosylated *in vivo*. Peptide-*N*-glycosidase treatment of mouse hypothalamus extracts revealed that endogenous Gpr176 undergoes *N*-glycosylation. Using a heterologous expression system, I then obtained evidence that *N*-glycosylation occurs at four conserved asparagine residues in the N-terminal region of mouse Gpr176 (N4, N11, N17 and N26). Prevention of *N*-glycosylation by the mutation of these sites led to a drastic reduction in the Gpr176 protein level. The non-glycosylated mutant proteins were mostly retained in the endoplasmic reticulum

(ER) and readily degraded via the proteasomal pathway, indicating that the non-glycosylated protein undergoes ER-associated degradation (ERAD). At the molecular function level, Gpr176 has constitutive, agonist-independent activity that leads to reduced cAMP synthesis. Although deficient *N*-glycosylation did not compromise this intrinsic activity, the resultant reduction in the Gpr176 protein expression on the plasma membrane was accompanied by attenuation of cAMP-repressing activity in cells. My data therefore demonstrate that *N*-glycosylation is a prerequisite for the efficient protein expression of functional Gpr176.

Chapter 2: Identification of regulation of Gpr176 activity via phosphorylation by T-207219 and other non-orphan GPCRs.

Phosphorylation is a key regulatory post-translational modification described for GPCRs. In canonical GPCR-mediated signaling pathway, agonist-activated receptors are phosphorylated in their cytoplasmic regions, resulting in subsequent receptor internalization and degradation. However, little is known about phosphorylation and its potential function(s) for orphan GPCRs. Because unlike other GPCRs, Gpr176 has a relatively large cytoplasmic C-terminal cytoplasmic tail region composed of 181 amino acids, where several phosphorylatable serine/threonine residues are conserved, it is tempting to speculate that this region may be involved in the regulation of Gpr176 via phosphorylation.

In the 2nd chapter, I describe the identification and characterisation of phosphorylation that occurs on Gpr176. Using a high-throughput chemical library screening, I first identified T-207219 as a regulator for Gpr176, which induces phosphorylation at two separate conserved serine residues in the C-terminal region of Gpr176, causing receptor internalization and degradation. Moreover, using a receptor co-expression system, I obtained evidence that ligand-mediated activation of non-orphan GPCRs leads to phosphorylation of the same residues in Gpr176. Induced phosphorylation, importantly, caused reduced cell-surface expression and second messenger signaling of Gpr176. My data therefore identified a previously uncharacterised inter-GPCR mechanism in which the orphan receptor is regulated by non-orphan receptors through phosphorylation.

Based on the results from **Chapters 1 and 2**, I have, for the first time, identified biochemical features of Gpr176 and discovered that the level of Gpr176 activity is regulated by post-translational modifications. My findings therefore provide an important basis for understanding GPCR regulation in the SCN and for developing Gpr176-targeted therapeutics.

Chapter 1

Identification and functional characterisation of *N*-linked glycosylation of the orphan G protein-coupled receptor Gpr176

INTRODUCTION

GPCRs are the largest family of cell-surface receptors and are the therapeutic targets of nearly a third of clinically marketed drugs[1,2]. Despite their importance, more than one hundred human GPCRs remain poorly characterised due to the lack of useful information on their ligands[3]. Included among these so-called orphan GPCRs is Gpr176, which is predicted to be a 56-kDa seven-transmembrane protein of class A GPCR with potential sites for *N*-glycosylation.

GPR176 (also known as *HB-954*) was initially cloned from a human brain cDNA library by Hata *et al.*[4]. In the mouse brain, the *Gpr176* mRNA level is predominantly high in the SCN of the hypothalamus[5], the principal circadian pacemaker in mammals, and knockout studies have shown that *Gpr176* is required to set the pace of circadian rhythm in behaviour[5]. This gene is also expressed in tissues other than the brain[4] and was reported to be involved in the anacardic acid-induced transcriptional response of human breast cancer cells[6]. Gpr176 couples to G_z, a subtype of $G_{i/o}$, and even in the absence of a known ligand, Gpr176 possesses an agonist-independent constitutive activity that leads to reduced cAMP synthesis[5,7]. At the amino acid sequence level, Gpr176 contains five extracellular potential sites for *N*-glycosylation (Asn-X-Ser/Thr, where X is any amino acid except for Pro); one is located in the third extracellular loop (ECL3) and the other four are located in the N-terminal region. However, whether these sites indeed undergo *N*-glycosylation remains unknown.

Not surprisingly, knowledge regarding the presence and potential functional role(s) of the *N*-glycosylation of orphan GPCRs has been particularly sparse relative to that of receptors with known ligands. Previous studies based on receptors with known ligands demonstrated that the functional role(s) of *N*-glycosylation varied depending on the type of GPCRs tested[8-26].

N-glycosylation of GPCRs may be important for their structural maturation, cell surface expression, ligand binding, and downstream signal transduction[8-27]. Because of the nonredundant functional nature of *N*-glycosylation, its role for the orphan GPCR Gpr176 must be determined empirically. It is also known that *N*-glycosylation occurs co-translationally—that is, during protein synthesis—in the lumen of the endoplasmic reticulum (ER)[28-32].

Here, I describe the identification and characterisation of *N*-linked glycosylation of the orphan receptor Gpr176. I show that Gpr176 is *N*-glycosylated *in vivo* in the mouse SCN. Using a heterologous expression system, I show that *N*-glycosylation occurs at four conserved asparagine residues in the N-terminal region of mouse Gpr176 (N4, N11, N17, N26). Prevention of *N*-glycosylation by the mutation of these sites led to a drastic reduction in the Gpr176 protein level and the non-glycosylated mutant proteins were mostly retained in the ER, indicating that non-glycosylated Gpr176 undergoes ER-associated degradation (ERAD) during protein biosynthesis. At the molecular level, deficient *N*-glycosylation did not impair the constitutive activity of Gpr176. Nevertheless, the reduction in Gpr176 protein expression caused by lack of *N*-glycosylation led to reduced total cAMP-repressive activity in the cells. I show that *N*-glycosylation is a prerequisite for the maximal protein expression of functional Gpr176.

EXPERIMENTAL PROCEDURES

Mouse hypothalamic membrane protein samples

All animal experiments were conducted in compliance with ethical regulations in Kyoto University and performed under protocols approved by the Animal Care and Experimentation Committee of Kyoto University. The brain hypothalamus was collected from C57BL/6 male WT mice or C57BL/6-backcrossed *Gpr176*$^{-/-}$ mice[5] and homogenized with a Dounce tissue grinder in a hypotonic buffer containing 20 mM HEPES (pH7.8), 2 mM EDTA, 1 mM DTT, and 1×cOmplete Protease Inhibitor cocktail (Roche Diagnostics). After centrifugation at 20,400×*g* for 30 min, the pellet was resuspended in a high-salt buffer containing 500 mM NaCl, 20 mM HEPES (pH7.8), 2 mM EDTA, 1 mM DTT, and 1×cOmplete Protease Inhibitor cocktail. The mixture was then centrifuged, and the resultant pellet was solubilized with a detergent-containing buffer (20 mM HEPES [pH7.8], 150 mM NaCl, 2 mM EDTA, 1 mM DTT, 1% cholesteryl hemisuccinate, 0.2% dodecyl-β-D-maltoside, and 1×cOmplete Protease Inhibitor). The soluble fractions were either subjected to glycosidase treatment (see below for details) or denatured in Laemmli buffer for immunoblot analysis. All procedures were carried out at 4°C.

Flp-In TREx 293 cell cultures and treatments

Flp-In TREx293-Gpr176 (tet-on) cells were generated by stable transfection of Flp-In T-REx 293 cells (Thermo Fisher Scientific) with a pcDNA5/FRT vector containing the untagged full-length coding sequence of the mouse *Gpr176* (NM_201367). Point mutations at the potential *N*-glycosylation sites (N4, N11, N17, N26, N295) were generated by substituting asparagine (N) to glutamine (Q) with a standard sequential PCR method[33]. To generate Gpr176-GFP, the entire coding sequence of Gpr176 without stop codon was fused in frame

to the N-terminus of GFP. To create Flp-In TREx293-Gpr176 (tet-on)/GloSensor (constitutive) cells, I constructed a modified pcDNA5/FRT vector carrying Gpr176 and GloSensor-22F (Promega) under different promoters: while *Gpr176* was cloned into a proprietary pcDNA5/FRT cloning site for tet-on induction, *GloSensor* was cloned separately into a different position of the vector (at a unique *Pci*I site) in conjunction with a tet-insensitive CMV promoter. Cells were cultured, unless otherwise specified, at 37°C under 5% CO_2 in DMEM medium (Nacalai, #08458-16) containing 10% fetal bovine serum, 100 μg ml^{-1} hygromycin, 10 μg ml^{-1} blasticidin, and 1% Antibiotic-Antimycotic Mixed solution (Nacalai). For Dox treatment, doxycycline (Clontech Laboratories) was added to the medium to a final concentration of 1 μg ml^{-1}. Where indicated, MG132 (Calbiochem) or bafilomycin A1 (Sigma) was added to the culture medium after 15 h of Dox treatment.

Glycosidase treatment

Peptide-*N*-glycosidase F (PNGase F) and *O*-glycosidase were purchased from New England BioLabs and used according to the manufacturer's instructions. Membrane fractions of Flp-In TREx293 (tet-on) cells or SCN extracts were incubated with a mixture of cholesteryl hemisuccinate (1%) and dodecyl-β-D-maltoside (0.2%), and their soluble fractions were denatured using 1×Glycoprotein Denaturing Buffer (New England BioLabs) for 5 min at 70°C. After chilled on ice, the denatured proteins were incubated with PNGase F (50 U μl^{-1}) or *O*-glycosidase (400 U μl^{-1}) in 1×G7 Reaction Buffer (New England BioLabs) supplemented with 1% NP-40 for 2 h at 37°C. The reaction was stopped by Laemmli buffer for the subsequent analysis.

Immunoblotting

Immunoblotting was performed using our standard method[34] with affinity-purified antibody against Gpr176. Gpr176 antiserum was acquired in rabbit using a glutathione-*S*-transferase (GST)-fused Gpr176 mouse protein fragment (amino acids (a.a.) 311–515)[5]. The affinity-purified Gpr176 antibody used in this study was re-prepared from the same batch of the antiserum using a maltose-binding protein (MBP)-fused Gpr176 fragment (a.a. 311–515). Antibodies for β-actin (Sigma, A5441) and Hsp70 (Santa Cruz, sc-66048) were also used for internal control.

RNA extraction and qRT-PCR

Total RNA was extracted with RNeasy kit (Qiagen) and converted to cDNA with SuperScript VILO cDNA Synthesis kit (Thermo Fisher Scientific). Real-time PCR was performed using THUNDERBIRD SYBR qPCR Mix (TOYOBO) on a StepOnePlus Real-Time PCR System (Thermo Fisher Scientific). Control primers for *RPLP0* (NM_053275) were F (5′-ATG CAG CAG ATC CGC ATG T-3′) and R (5′-TTG CGC ATC ATG GTG TTC TT-3′), and primers for *Gpr176* (NM_201367) were F (5′-CAT CTT CAT TGG CTC GCT AC-3′) and R (5′- CGT ATA GAT CCA CCA GCA AC-3′).

Fluorescence microscopy

Flp-In TREx293 Gpr176-GFP (tet-on) cells and the related cells that express an N-terminal *N*-glycosylation mutant Gpr176-GFP were plated on polylysine-coated coverslips in culture medium containing 1 μg ml^{-1} Dox for 15 h. The cells were fixed with 4% paraformaldehyde and mounted in ProLong Gold antifade reagent with DAPI (Thermo Fisher Scientific). The Gpr176 GFP fusion protein subcellular localization was monitored using direct fluorescence from the GFP moiety. For ER staining, cells were treated with 1 μM ER-Tracker Red

(Thermo Fisher Scientific). ER-Tracker is a fluorescence-labeled glibenclamide that is capable of visualizing ER via specific binding to the sulphonylurea receptors of ATP-sensitive K^+ channels, which are prominent on ER[35]. For calnexin immunodetection, the cells were fixed, permeabilized, and blocked with 5% bovine serum albumin in PBS containing 0.1% Triton X-100, as described[36]. The cells were immunolabeled with anti-calnexin (BD Transduction Laboratories, #610523) and visualized with Alexa594-conjugated anti-mouse IgG (Thermo Fisher Scientific). Images were captured using an Olympus FV10I-DOC confocal microscope.

GloSensor-cAMP assay

Flp-In TREx293-Gpr176 (tet-on)/GloSensor (constitutive) cells and the related cells that express an *N*-glycosylation-deficient Gpr176 were seeded in a collagen I-coated 96-well plate (Corning) at a density of 5.4×10^4 cells per well with a carbon dioxide-independent DMEM medium (Sigma, D2902) containing 10% bovine serum, 0.035% sodium bicarbonate, 10 mM HEPES (pH 7.2), 3.5 g l^{-1} D-glucose, and 1% Antibiotic-Antimycotic Mixed solution (Nacalai). D-Luciferin (Promega) was also included in the medium at a concentration of 1mM. After 6 h at 37°C, the cells received Dox (final, 1 μg ml^{-1}) or vehicle and underwent additional incubation at 37°C for 15 h. Prior to luminescence detection, the cell culture plate was acclimatized to 27°C for 1 h. Luminescence was then recorded on a FDSS/μCELL plate reader (Hamamatsu Photonics) at 27°C every 5 sec. Forskolin (final, 10 μM) was added to the culture medium 2 minutes after the start of measurement. Data were integrated over 1-min or 30-sec intervals, and the values were normalized to the average peak luminescence of Dox (−) cells.

For the verification of intracellular total GloSensor levels in Dox-treated and non-treated cells, cells were lysed into a passive lysis buffer (Promega) with a volume of 100 µl per well, and aliquots of the lysates were mixed with or without cAMP (final, 1 or 4 µM) and assayed for GloSensor activity using a Luciferase Assay Reagent II (Promega).

cAMP enzyme immunoassay

Intracellular cAMP levels were determined by enzyme immunoassay (EIA). Cells were lysed into 6% perchloric acid solution containing 4 mM theophylline (Sigma) at 4°C and neutralized with 0.72 M KOH / 0.6 M $KHCO_3$. After removal of salt precipitates, the extracts were subjected to an EIA for cAMP using a kit purchased from Cayman Chemical (Cat. No 581001)[5,37].

Glycosidase-treated cell suspension GloSensor assay

Cells of the same batch were cultured in parallel with or without Dox (1 µg ml^{-1}) for 15 h and then removed from dish with Versene solution (Life Technologies). Cells were dissociated into single cells through gentle trituration and filtered via a 70-µm cell strainer (BD Falcon). Cells were resuspended in HBSS containing 5 mM HEPES (pH7.5) and 0.1% bovine serum albumin at a cell density of 8×10^6 cells/ml. The suspensions were then immediately treated with PNGase F (5 U μl^{-1}) or vehicle for 1 h at 37°C with gentle agitation. Following enzymatic depletion of *N*-linked glycosylation, cells were transferred into fresh HBSS containing 5 mM HEPES (pH7.5), 0.1% bovine serum albumin, and 1 mM luciferin, and cells in suspension (~1×10^5 cells per well) were assayed for GloSensor activity. Data were normalized with total GloSensor levels, for which cell lysates were incubated with excess cAMP.

RESULTS

Gpr176 undergoes *N*-glycosylation *in vivo*

The presence of the consensus *N*-glycosylation sequences (Asn-X-Ser/Thr, where X is not Pro) in Gpr176 (**Fig. 1A**) prompted me to ask whether Gpr176 is glycosylated *in vivo*.

Western blotting of endogenous Gpr176 in the mouse hypothalamic SCN extract using an antibody against Gpr176, which was raised against the C-terminal intracellular region of mouse Gpr176, revealed a broad band migrating at around 75 kDa. The band at around 75kDa was not detected in the SCN extract prepared from *Gpr176*$^{-/-}$ mice (**Fig. 1B**), confirming the specificity of the antibody. Treatment of the SCN extract with PNGaseF resulted in a band shift toward ~50 kDa (**Fig. 1B, C**), which is consistent with the molecular mass predicted from the amino acid sequence. *O*-glycosidase treatment, which digests *O*-linked sugars, had little or no apparent effect on the Gpr176 mobility upon SDS-PAGE. These results together indicate that Gpr176 undergoes *N*-linked, but not *O*-linked, glycosylation.

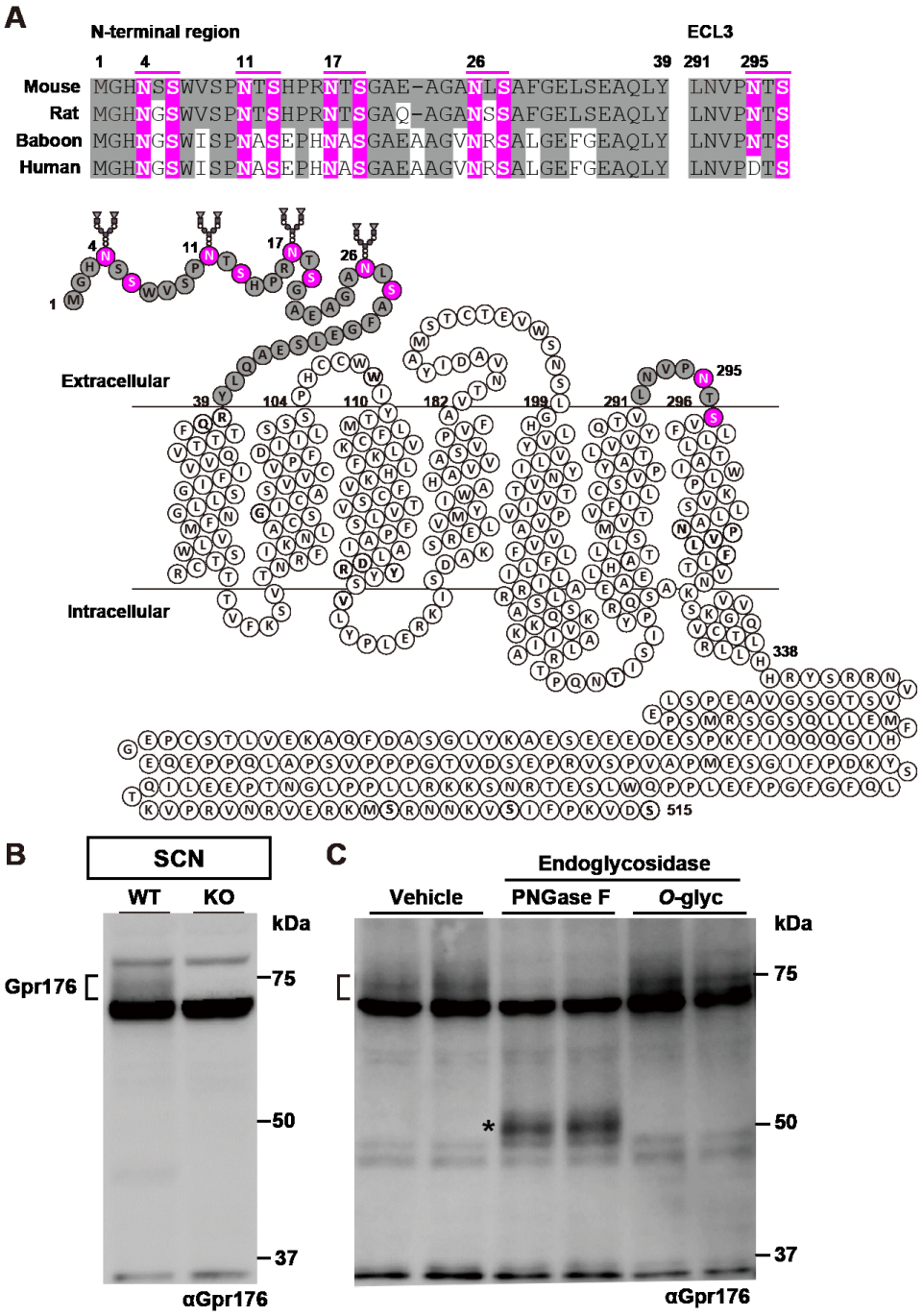

Fig. 1 | Gpr176 is an *N*-glycosylated GPCR. (**A**) Amino acid sequence conservation of the potential *N*-glycosylation sites in the N-terminal and extracellular loop 3 (ECL3) region of mouse, rat, baboon, and human Gpr176. Sequences that match the consensus *N*-linked glycosylation motif (N-X-S/T, where X is not P) are highlighted in magenta in the alignments as well as in the snake-plot representation of mouse Gpr176. (**B, C**) Immunoblot analysis of mouse hypothalamus SCN cell extracts from WT and *Gpr176*$^{-/-}$ mice for Gpr176 (**B**). The WT extracts were treated with vehicle or either PNGase F or *O*-glycosidase (*O*-glyc) and immunoblotted for Gpr176 (**C**). Two independent biological replicates per condition were loaded in (**C**). Note that a broad, heterogeneous band with an apparent molecular mass of 75 kDa was detectable only in the WT extract. The asterisk indicates the position of deglycosylated Gpr176.

***N*-glycosylation occurs in the N-terminal region of Gpr176**

Similar to endogenous Gpr176, exogenously expressed mouse Gpr176 in human embryonic kidney (HEK)293-derived Flp-In T-REx 293 cells displayed an apparent molecular mass of ~75 kDa, which was shifted down to ~50 kDa by PNGase F treatment (**Fig. 2A**), indicating that exogenously expressed Gpr176 underwent *N*-glycosylation in a manner similar to that occurring *in vivo*.

Site-directed mutagenesis of individual potential *N*-glycosylation sites implicated that all four consensus sites in the N-terminal region of Gpr176 (N4, N11, N17, and N26) are glycosylated (**Supplementary Fig. 1**). Thus, I generated a mutant Gpr176 protein harbouring simultaneous Asn (N) to Gln (Q) substitutions of all the N-terminal consensus *N*-glycosylation sites (N4Q, N11Q, N17Q, and N26Q), designated hereafter as N-ter mut. N-ter mut and wild-type (WT) Gpr176 were expressed in Flp-In TREx293 cells in a doxycycline (Dox)-inducible manner. Immunoblot analysis of Dox-treated (+) and -untreated (−) cells revealed that the apparent molecular mass of the mutant Gpr176 protein that appeared after Dox treatment (indicated by a solid arrowhead in **Fig. 2B**) was ~50 kDa, which was approximating to the size of PNGase F-treated WT Gpr176 (**Fig. 2A**).

In addition to the change in size, I noticed that the removal of the N-terminal glycosylation sites caused a drastic reduction in the total protein level of Gpr176, compared with the level of β-actin as a loading control (**Fig. 2B**). At the mRNA level, the expression of N-ter mut was comparable to WT Gpr176 (**Fig. 2C**). By contrast, the mean protein expression level of N-ter mut was reduced to less than 10% of that of WT (**Fig. 2D**), necessitating extended exposure for immunoblot detection (**Fig. 2B**). I found the apparent molecular mass of the other mutant, which lacks the potential *N*-glycosylation site in the third extracellular loop

(ECL3), to be ~75 kDa and its protein level to be comparable to that of WT Gpr176 (**Fig. 2B–D**). By contrast, combinational mutations of the N-terminal and ECL3 sites reproduced the reduction in size and in the protein level of Gpr176 (**Fig. 2B–D**, N-ter/ECL3). These results indicate that N-terminal *N*-glycosylation is required for the proper protein expression of Gpr176.

Additionally, I noticed that in cells in which Gpr176 was overexpressed, a minor fraction of the WT proteins migrated at approximately 50 kDa (**Fig. 2B**; open arrowhead), which possibly reflects the presence of immature or less glycosylated proteins, as reported for other GPCRs and non-GPCR glycoproteins that have been overexpressed.

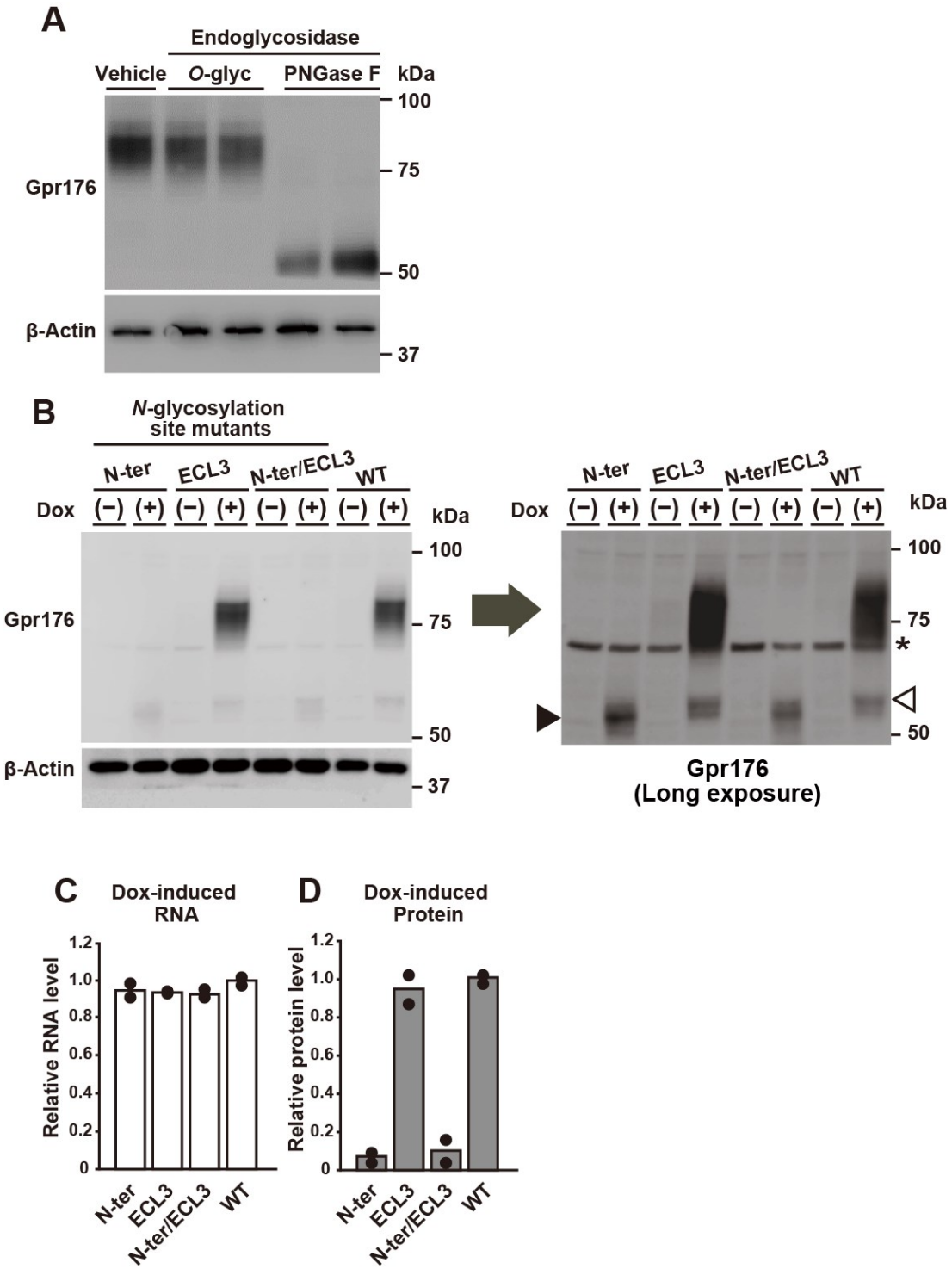

(Legend on next page)

Fig. 2 | *N*-glycosylation in the N-terminal region is required for the optimal expression of Gpr176. (**A**) *N*-glycosylation of Gpr176 exogenously expressed in Flp-In TREx293 cells. Dox-treated Flp-In TREx293-Gpr176 (tet-on) cell extracts were treated with PNGase F or *O*-glyc and immunoblotted for Gpr176 (upper) and β-actin (lower). (**B**) Immunoblots of Dox-treated (+) and untreated (−) Flp-In TREx293 (tet-on) cells expressing WT Gpr176 and the respective mutants for potential *N*-linked glycosylation sites: N-ter (N4, 11, 17, 26Q), ECL3 (N295Q), and N-ter/ECL3 (N4, 11, 17, 26, 295Q). The same membrane exposed for a longer time is shown on the right. A closed arrowhead indicates the position of the proteins with an N-ter mutation. An open arrowhead points to a minor fraction of Dox-induced WT proteins. Asterisk, nonspecific bands. (**C**, **D**) Dox-induced mRNA (**C**) and protein (**D**) expression levels of WT Gpr176 and the N-ter, ECL3, and N-ter/ECL3 Gpr176 mutants. Relative *Gpr176* mRNA levels were determined by qRT-PCR and normalized to the expression levels of the gene encoding the ribosomal phosphoprotein P0. For the protein level, relative band intensities in blots exposed for a longer time (**B**) were determined using densitometry. Data are represented as the mean of two independent experiments with variation.

N-glycosylation is a prerequisite for the proper cell surface expression of Gpr176

To test the effect of deficient *N*-glycosylation on the subcellular localization of Gpr176, I examined a Flp-In TREx293 cell line expressing GFP-fused Gpr176 (**Fig. 3**). GFP was fused to the C-terminal end of Gpr176. Confocal microscopy revealed that the WT Gpr176-GFP fluorescence was distributed mostly on the plasma membrane (**Fig. 3A**), congruent with the reported plasma membrane immunolocalization of untagged Gpr176. Attenuated N-ter mut protein expression was also observed for the mutant protein fused to GFP (**Supplementary Fig. 2**). The corresponding GFP signals were therefore intensified when imaging the subcellular localization of the mutant. I found that, under these conditions, the fluorescent signals of the N-ter mut were more intense in the perinuclear region corresponding to the ER than on the plasma membrane (see **Fig. 3A,B** and **Supplementary Fig. 3**), suggesting an impairment in maturation and export from the ER of the non-glycosylated protein. Total protein levels of mutant Gpr176 were partly restored by treatment of the cells with MG132 (a proteasome inhibitor) but not with bafilomycin A1 (a lysosomal inhibitor) (**Fig. 3C, D**). Similar results were observed in experiments using untagged Gpr176 (**Supplementary Fig. 4**). These results indicate that the majority of the non-glycosylated Gpr176 is retained in the ER and undergoes ERAD via the proteasomal pathway.

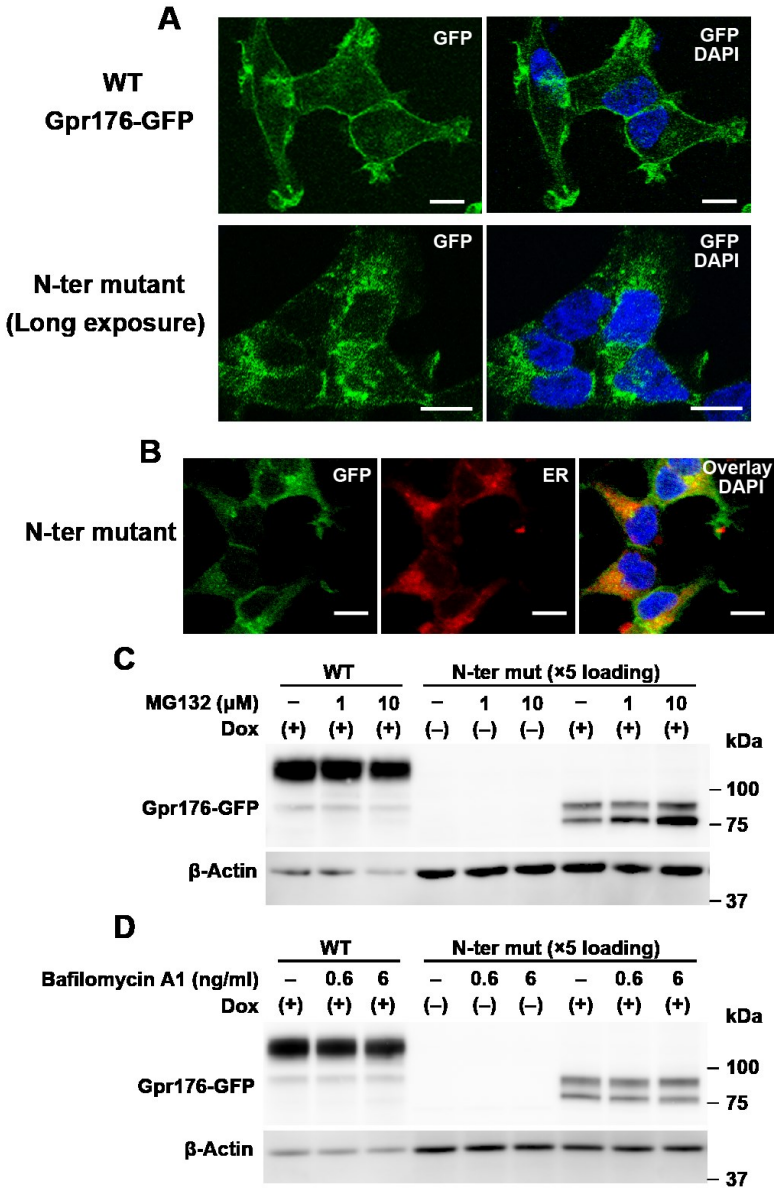

Fig. 3 | The prevention of *N*-glycosylation leads to reduced cell surface expression of Gpr176. (**A**) Representative confocal images of Flp-In TREx293 cells expressing WT (upper) or N-ter mut Gpr176-GFP (lower). Merged are combined image of GFP (green) and DAPI for the nucleus (blue). Gamma levels were adjusted over the whole image to optimize the appropriate GFP signals. The images are representative of three independent experiments. Scale bars, 10 μm. (**B**) Confocal images showing intracellular accumulation of N-ter mut Gpr176-GFP (green) in ER. Cells were stained with ER-tracker (red). The merged image is a combined image with DAPI (blue). Cells are representative of a population with independent experiments repeated four times. Scale bars, 10 μm. (**C**,**D**) Immunoblot analysis examining the effect of MG132 (**C**) and bafilomycin A1 (**D**) treatment on the level of WT and N-ter mut Gpr176-GFP. Cells were treated with MG132 (**C**) or bafilomycin A1 (**D**) at the indicated concentrations for 6 h. The extract of N-ter mutant cells were loaded at five-fold higher level compared to that of WT cells to detect the lower level of the protein. Note that the N-ter mut level was partially restored by the MG132 (**C**) but not by bafilomycin A1 (**D**) treatment, while WT expression was nearly unchanged by both treatments.

Attenuated N-ter mut expression is accompanied by reduced total activity of Gpr176

In agreement with previous reports, Dox-induced expression of WT Gpr176 led to the attenuation of forskolin (Fsk)-induced intracellular cAMP accumulation (**Fig. 4**), confirming that this orphan receptor has constitutive, agonist-independent activity. Changes in the intracellular cAMP level were assayed using either a luciferase-based cAMP biosensor (GloSensor 22F) that was stably incorporated into the cells (**Fig. 4A**) or a cAMP enzyme-immunoassay (EIA). As observed in **Fig. 4B–D**, regardless of the type of assay method used, the amplitude of cAMP accumulation was significantly attenuated by ~30% in Dox-treated (+) cells versus untreated (−) cells ($P < 0.001$ for the GloSensor assay, $P < 0.05$ for EIA, two-tailed unpaired *t*-test), suggesting that the GloSensor assay and EIA were equivalent in their ability to detect Gpr176-derived cAMP-repressive activity in the cells (see also **Supplementary Fig. 5**).

Using the GloSensor assay, I then evaluated the functional consequence of attenuated protein expression of glycosylation-deficient N-ter mut Gpr176. I observed that cells expressing N-ter mut still exhibited measurable cAMP-repressive activity, albeit with a significantly diminished amplitude compared to that of cells expressing WT Gpr176 (see **Fig. 4E,G**, $P < 0.0005$, WT versus N-ter mut, one-way ANOVA, Bonferroni test). Although it may be argued that *N*-glycosylation has a direct effect on the molecular function of Gpr176, there is another possible interpretation of this result. Since the activity was measured in cells (see **Supplementary Fig. 6**), the observed decrease in cAMP-repressive activity might reflect the reduced protein level of the mutant in cells. I also showed that, in contrast to cells expressing N-ter mut, those expressing the ECL3 mutant had normal cAMP-repressive activity, which was indistinguishable from that of WT Gpr176-expressing cells (**Fig. 4F,G**).

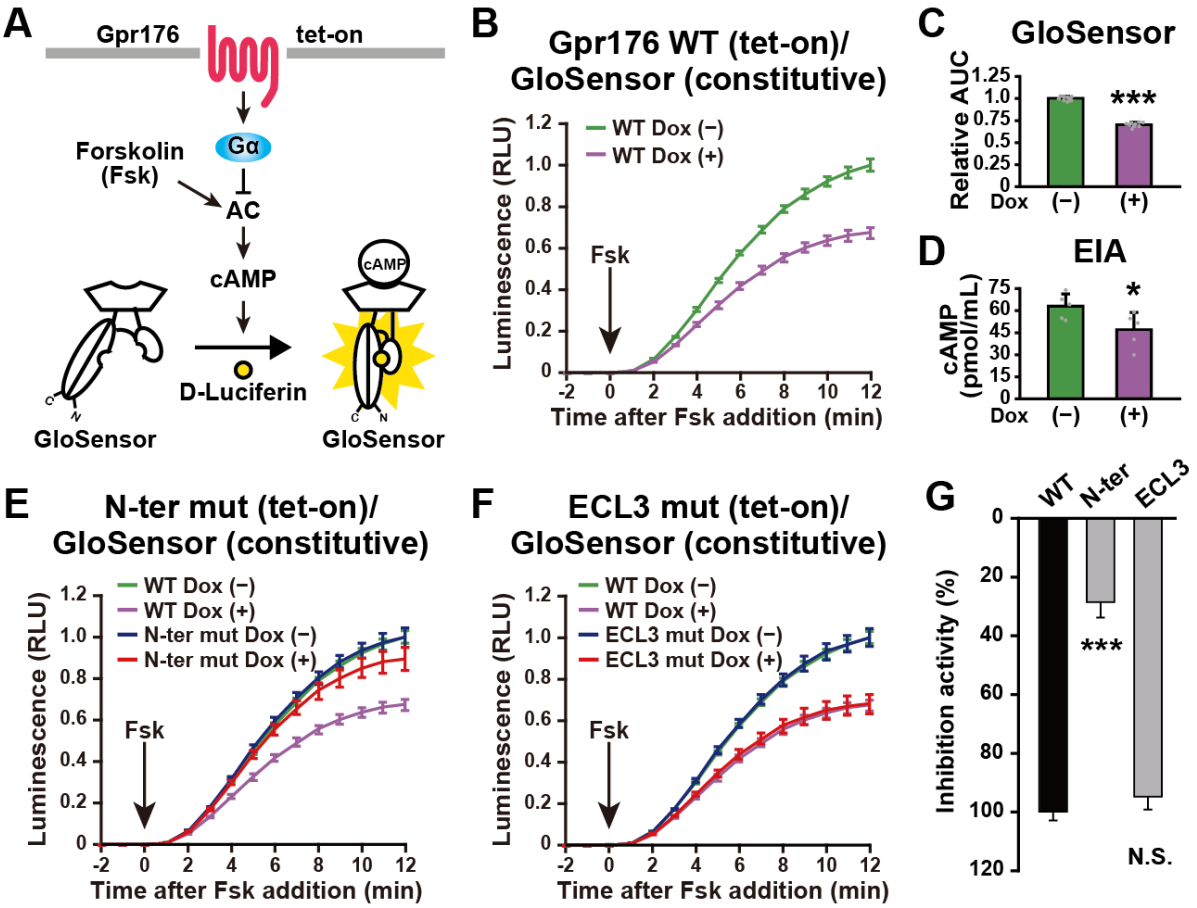

Fig. 4 | Attenuated expression of the glycosylation mutant results in reduced total activity of Gpr176. (**A**) Experimental design based on Flp-In TREx293-Gpr176 (tet-on)/ GloSensor (constitutive) cells. (**B**) Forskolin (Fsk)-induced cAMP GloSensor luciferase activity traces in Dox-treated (+) and untreated (−) Flp-In TREx293-Gpr176 (tet-on)/GloSensor (constitutive) cells. The arrow indicates the start of Fsk treatment. RLU, relative light units. Values (means ± s.d., $n = 9$ for each data point) are plotted relative to the average peak value obtained in untreated cells. (**C**) Relative area under the curve (AUC) of luminescence values in (**B**). Light emissions were integrated and normalized with those of the untreated control. ***$P < 0.0005$, two-tailed unpaired t-test ($n = 9$ for each condition). Error bars indicate s.d. (**D**) Intracellular cAMP concentrations determined by cAMP enzyme immunoassay (EIA). *$P < 0.05$, two-tailed unpaired t-test ($n = 5$ for each condition). Error bars indicate s.d. (**E**) GloSensor activity traces in Dox-treated (+) and untreated (−) Flp-In TREx293 N-ter mut Gpr176 (tet-on)/GloSensor (constitutive) cells. For comparison, the GloSensor traces of WT cells (replots of **B**) are displayed in parallel. Values are the means ± s.d. ($n = 9$). (**F**) GloSensor traces in Dox-treated (+) and untreated (−) Flp-In TREx293 ECL3 mut Gpr176 (tet-on)/GloSensor (constitutive) cells. The traces of WT cells (**B**) are shown in parallel. Values are the means ± s.d. ($n = 9$). (**G**) Percent cAMP-inhibitory activities of N-ter and ECL3 mut Gpr176 relative to that of WT Gpr176. The AUC was used to evaluate the rate of cAMP inhibition. The values are plotted as a percent relative to WT Gpr176 (100%). Data are the means ± s.e.m. of nine replicates each. ***$P < 0.0005$ versus WT, one-way ANOVA with Bonferroni *post hoc* test. N.S., not significant.

N-glycosylation is not essential for the basal activity of Gpr176

Because prevention of the *N*-glycosylation of Gpr176 resulted in a drastic reduction in the protein level, site-directed mutagenesis may not be appropriate to address the role of *N*-glycosylation in the molecular function of Gpr176. To circumvent this inherent problem, I turned to a different approach. As shown in **Fig. 5A**, cells underwent deglycosylation treatment before Gpr176 activity was assayed. Freshly dissociated Dox-treated (+) and untreated (−) cell suspensions were treated with or without PNGase F for 1 h. Following the enzymatic depletion of *N*-linked glycosylation, cells were immediately assayed for forskolin-induced changes in GloSensor activity (**Fig. 5B**). Western blotting (**Fig. 5C**) demonstrated that the PNGase F treatment caused a down-shift of the Gpr176 band but did not alter the protein level of Gpr176. Under these conditions, I found that deglycosylated Gpr176 retained an essentially unimpaired ability to reduce cAMP accumulation ($P < 0.0005$, for both PNGase F (−) and (+) conditions, see **Fig. 5B**). These data suggest that *N*-glycosylation is not an absolute requirement for the agonist-independent constitutive function of Gpr176.

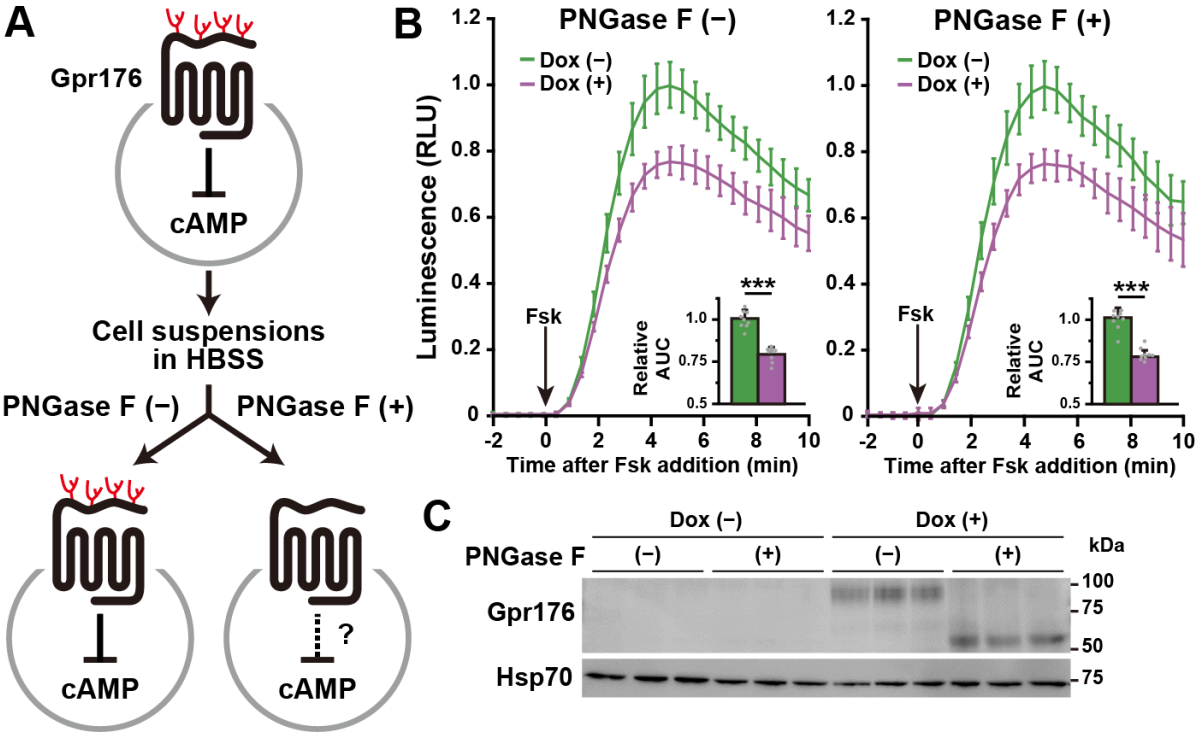

Fig. 5 | PNGase F-treated Gpr176 retains its cAMP-repressive activity. (**A**) Schematic experimental design for the glycosidase-treated cell suspension GloSensor assay. Dox-treated (+) and untreated (−) cells were resuspended in HBSS with or without PNGase F for 1 h before the GloSensor cAMP assay. (**B**) Fsk-induced GloSensor activity traces in PNGase F-treated and untreated Flp-In TREx293-Gpr176 (tet-on)/GloSensor (constitutive) cell suspensions. The arrow indicates the start of Fsk treatment. RLU, relative light units. Values (means ± s.d., $n = 9$ for each data point) are plotted relative to the average peak value obtained in Dox-untreated cells. Insets indicate relative AUC values (means ± s.d., $n = 9$; ***$P < 0.0005$, two-tailed unpaired t-test). (**C**) Immunoblots of representative PNGase F-treated and untreated Flp-In TREx293-Gpr176 (tet-on)/ GloSensor (constitutive) cells. The cell suspension samples were immunoblotted for Gpr176 (upper) and Hsp70 as a loading control (lower).

DISCUSSION

N-glycosylation is one of the most common posttranslational modifications of membrane protein GPCRs, yet literature regarding the presence and potential functional roles of *N*-glycosylation of orphan GPCRs remains sparse. In the present study, I identified and characterised *N*-glycosylation of the orphan GPCR Gpr176. Importantly, the functional significance of *N*-glycosylation differs between GPCRs (see ref. 8−27). In the case of Gpr176, *N*-glycosylation is required for its efficient cell-surface expression. However, this does not necessarily hold true for other GPCRs. The orphan GPCR Gpr61 was reported to be *N*-glycosylated[27], but *N*-glycosylation is not vital for its protein level[27]. Similarly, it was shown that the expression level of the α_1-adrenergic receptor[8], M_2 muscarinic receptor[9], histamine H_2 receptor[10], vasopressin V_2 receptor[11], PTH receptor[12], LH-RH receptor[13], or oxytocin receptor[14] was not significantly modified by the depletion of *N*-glycosylation, while those of rhodopsin[15], β_2-adrenergic receptor[16], and angiotensin II type-1 receptor[17] were all reduced, akin to Gpr176. Moreover, depending on the type of receptor examined, *N*-glycosylation can be either critical or not critical for GPCR function. For example, *N*-glycosylation of the vasopressin V1a receptor is critical to maintain optimal ligand binding affinity[25] and *N*-glycosylation of $P2Y_{12}$ receptor is required to induce proper downstream G_i-mediated signalling[26]. By contrast, *N*-glycosylation is not needed for the receptor functions of rhodopsin[15], histamine H_2 receptor[10], and angiotensin II type-1 receptor[17]. Because of these versatile and non-uniform effects of *N*-glycosylation, it has been widely acknowledged that the role of the *N*-glycosylation of specific GPCRs must be determined empirically[23]. In this regard, to the best of my knowledge, Gpr176 is the first orphan GPCR whose *N*-glycosylation has been verified to be indispensable for proper protein expression. *N*-glycosylation is not essential for the molecular function of Gpr176. However, deficient *N*-

glycosylation caused a drastic reduction in the protein level and thereby led to reduced total cAMP-repressive activity in the cells. Thus, *N*-glycosylation is likely a prerequisite for the proper protein expression of functional Gpr176.

Pharmacological treatment indicated that MG132, but not bafilomycin A1, partially restored the cellular level of the non-glycosylated N-ter mut Gpr176, while the level of WT Gpr176 was not substantially increased by either MG132 or bafilomycin A1. I also observed accumulation of deglycosylated Gpr176 in the ER, where GPCRs are normally synthesised and *N*-glycosylated[28-32]. These lines of circumstantial evidence suggest that the absence of *N*-glycan modification destabilizes this protein, possibly due to improper folding that renders the protein susceptible to ER-associated quality control leading to proteasomal degradation[28-32]. Further investigation will be necessary to understand the precise mechanism underlying the reduced level of non-glycosylated Gpr176.

To date, over 330 non-synonymous SNPs (single nucleotide polymorphisms) have been identified in the human *GPR176* (*hGPR176*) (dbSNP, https://www.ncbi. nlm.nih.gov/). By characterizing all SNPs that are located in the conserved *N*-glycosylation motifs of hGPR176 (rs1473415441, rs1478819979, rs761894953, rs1293261954, and rs556899221), our laboratory previously showed that the variations N4S and S13G (SNPs rs1473415441 and rs761894953 respectively) attenuate the *N*-glycosylation level and thereby reduce protein expression level and cAMP-repressing activity[38,39]. These two SNPs are both rare genetic variants (minor allele frequency < 0.01%) with no previously reported association with (patho)physiology. Thus, currently, physiological contribution of *N*-glycosylation of GPR176 is completely unclear. Moreover, rare-variant effects cannot easily be identified via

genome-wide association studies (GWAS) because of the problem of statistical power. In this sense, however, it is interesting to note that a previous GWAS of 89,283 individuals identified *ALG10B*, a gene encoding an enzyme catalysing the formation of *N*-glycan, as being associated with human circadian behaviour[40]. Although the mechanism by which ALG10B affects the circadian clock system is unknown, it is tempting to speculate that ALG10B might modify the extent of *N*-glycosylation of hGPR176. I found that Gpr176 is *N*-glycosylated in the mouse hypothalamic SCN, a structure known to function as the master clock of the body. In addition, based on amino acid sequence analysis, other circadian clock-related GPCRs and non-GPCR proteins that operate in the SCN (such as GPCR Vipr2 and the ion channel NMDA receptor) may be *N*-glycosylated *in vivo*. Therefore, examining whether ALG10B-mediated *N*-glycan modifications affect the *in vivo* function and expression of Gpr176/GPR176 (and other GPCRs/non-GPCRs in the SCN) will be a focus of future study.

REFERENCES

1 Santos, R. *et al.* A comprehensive map of molecular drug targets. *Nat Rev Drug Discov* **16**, 19-34, doi:10.1038/nrd.2016.230 (2017).

2 Hauser, A. S., Attwood, M. M., Rask-Andersen, M., Schioth, H. B. & Gloriam, D. E. Trends in GPCR drug discovery: new agents, targets and indications. *Nat Rev Drug Discov* **16**, 829-842, doi:10.1038/nrd.2017.178 (2017).

3 Wacker, D., Stevens, R. C. & Roth, B. L. How Ligands Illuminate GPCR Molecular Pharmacology. *Cell* **170**, 414-427, doi:10.1016/j.cell.2017.07.009 (2017).

4 Hata, S., Emi, Y., Iyanagi, T. & Osumi, T. cDNA cloning of a putative G protein-coupled receptor from brain. *Biochim Biophys Acta* **1261**, 121-125 (1995).

5 Doi, M. *et al.* Gpr176 is a Gz-linked orphan G-protein-coupled receptor that sets the pace of circadian behaviour. *Nat Commun* **7**, 10583, doi:10.1038/ncomms10583 (2016).

6 Schultz, D. J. *et al.* Transcriptomic response of breast cancer cells to anacardic acid. *Sci Rep* **8**, 8063, doi:10.1038/s41598-018-26429-x (2018).

7 Martin, A. L., Steurer, M. A. & Aronstam, R. S. Constitutive Activity among Orphan Class-A G Protein Coupled Receptors. *PLoS One* **10**, e0138463, doi:10.1371/journal.pone.0138463 (2015).

8 Sawutz, D. G., Lanier, S. M., Warren, C. D. & Graham, R. M. Glycosylation of the mammalian alpha 1-adrenergic receptor by complex type N-linked oligosaccharides. *Mol Pharmacol* **32**, 565-571 (1987).

9 van Koppen, C. J. & Nathanson, N. M. Site-directed mutagenesis of the m2 muscarinic acetylcholine receptor. Analysis of the role of N-glycosylation in receptor expression and function. *J Biol Chem* **265**, 20887-20892 (1990).

10 Fukushima, Y. *et al.* Structural and functional analysis of the canine histamine H2 receptor by site-directed mutagenesis: N-glycosylation is not vital for its action. *Biochem J* **310 (Pt 2)**, 553-558, doi:10.1042/bj3100553 (1995).

11 Innamorati, G., Sadeghi, H. & Birnbaumer, M. A fully active nonglycosylated V2 vasopressin receptor. *Mol Pharmacol* **50**, 467-473 (1996).

12 Bisello, A. *et al.* Role of glycosylation in expression and function of the human parathyroid hormone/parathyroid hormone-related protein receptor. *Biochemistry* **35**, 15890-15895, doi:10.1021/bi962111+ (1996).

13 Davis, D. P., Rozell, T. G., Liu, X. & Segaloff, D. L. The six N-linked carbohydrates of the lutropin/choriogonadotropin receptor are not absolutely required for correct folding, cell surface expression, hormone binding, or signal transduction. *Mol Endocrinol* **11**, 550-562, doi:10.1210/mend.11.5.9927 (1997).

14 Kimura, T. *et al.* The role of N-terminal glycosylation in the human oxytocin receptor. *Mol Hum Reprod* **3**, 957-963, doi:10.1093/molehr/3.11.957 (1997).

15 Kaushal, S., Ridge, K. D. & Khorana, H. G. Structure and function in rhodopsin: the role of asparagine-linked glycosylation. *Proc Natl Acad Sci U S A* **91**, 4024-4028, doi:10.1073/pnas.91.9.4024 (1994).

16 Rands, E. *et al.* Mutational analysis of beta-adrenergic receptor glycosylation. *J Biol Chem* **265**, 10759-10764 (1990).

17 Deslauriers, B. *et al.* N-glycosylation requirements for the AT1a angiotensin II receptor delivery to the plasma membrane. *Biochem J* **339 (Pt 2)**, 397-405 (1999).

18 Servant, G., Dudley, D. T., Escher, E. & Guillemette, G. Analysis of the role of N-glycosylation in cell-surface expression and binding properties of angiotensin II type-2 receptor of rat pheochromocytoma cells. *Biochem J* **313 (Pt 1)**, 297-304, doi:10.1042/bj3130297 (1996).

19 Fan, G. *et al.* N-linked glycosylation of the human Ca2+ receptor is essential for its expression at the cell surface. *Endocrinology* **138**, 1916-1922, doi:10.1210/endo.138.5.5131 (1997).
20 Garcia Rodriguez, C. *et al.* The role of N-glycosylation for functional expression of the human platelet-activating factor receptor. Glycosylation is required for efficient membrane trafficking. *J Biol Chem* **270**, 25178-25184, doi:10.1074/jbc.270.42.25178 (1995).
21 Davidson, J. S. *et al.* Identification of N-glycosylation sites in the gonadotropin-releasing hormone receptor: role in receptor expression but not ligand binding. *Mol Cell Endocrinol* **107**, 241-245 (1995).
22 Michineau, S., Muller, L., Pizard, A., Alhenc-Gelas, F. & Rajerison, R. M. N-linked glycosylation of the human bradykinin B2 receptor is required for optimal cell-surface expression and coupling. *Biol Chem* **385**, 49-57, doi:10.1515/BC.2004.007 (2004).
23 Tansky, M. F., Pothoulakis, C. & Leeman, S. E. Functional consequences of alteration of N-linked glycosylation sites on the neurokinin 1 receptor. *Proc Natl Acad Sci U S A* **104**, 10691-10696, doi:10.1073/pnas.0703394104 (2007).
24 Roy, S., Perron, B. & Gallo-Payet, N. Role of asparagine-linked glycosylation in cell surface expression and function of the human adrenocorticotropin receptor (melanocortin 2 receptor) in 293/FRT cells. *Endocrinology* **151**, 660-670, doi:10.1210/en.2009-0826 (2010).
25 Lee, K. H. *et al.* Effect of N-glycosylation on ligand binding affinity of rat V1a vasopressin receptor. *Biochem Biophys Res Commun* **286**, 707-713, doi:10.1006/bbrc.2001.5456 (2001).
26 Zhong, X., Kriz, R., Seehra, J. & Kumar, R. N-linked glycosylation of platelet P2Y12 ADP receptor is essential for signal transduction but not for ligand binding or cell surface expression. *FEBS Lett* **562**, 111-117, doi:10.1016/S0014-5793(04)00191-7 (2004).
27 Kozielewicz, P. *et al.* N-glycosylation and expression in human tissues of the orphan GPR61 receptor. *FEBS Open Bio* **7**, 1982-1993, doi:10.1002/2211-5463.12339 (2017).
28 Cherepanova, N., Shrimal, S. & Gilmore, R. N-linked glycosylation and homeostasis of the endoplasmic reticulum. *Curr Opin Cell Biol* **41**, 57-65, doi:10.1016/j.ceb.2016.03.021 (2016).
29 Hebert, D. N., Lamriben, L., Powers, E. T. & Kelly, J. W. The intrinsic and extrinsic effects of N-linked glycans on glycoproteostasis. *Nat Chem Biol* **10**, 902-910, doi:10.1038/nchembio.1651 (2014).
30 Brodsky, J. L. Cleaning up: ER-associated degradation to the rescue. *Cell* **151**, 1163-1167, doi:10.1016/j.cell.2012.11.012 (2012).
31 Smith, M. H., Ploegh, H. L. & Weissman, J. S. Road to ruin: targeting proteins for degradation in the endoplasmic reticulum. *Science* **334**, 1086-1090, doi:10.1126/science.1209235 (2011).
32 Helenius, A. & Aebi, M. Roles of N-linked glycans in the endoplasmic reticulum. *Annu Rev Biochem* **73**, 1019-1049, doi:10.1146/annurev.biochem.73.011303.073752 (2004).
33 Cormack, B. Directed mutagenesis using the polymerase chain reaction. *Curr Protoc Mol Biol* **Chapter 8**, Unit8 5, doi:10.1002/0471142727.mb0805s37 (2001).
34 Doi, M. *et al.* Salt-sensitive hypertension in circadian clock-deficient Cry-null mice involves dysregulated adrenal Hsd3b6. *Nat Med* **16**, 67-74, doi:10.1038/nm.2061 (2010).

35 Hambrock, A., Loffler-Walz, C. & Quast, U. Glibenclamide binding to sulphonylurea receptor subtypes: dependence on adenine nucleotides. *Br J Pharmacol* **136**, 995-1004, doi:10.1038/sj.bjp.0704801 (2002).
36 Yamamura, K. *et al.* Immunolocalization of murine type VI 3beta-hydroxysteroid dehydrogenase in the adrenal gland, testis, skin, and placenta. *Mol. Cell. Endocrinol.* **382**, 131-138, doi:10.1016/j.mce.2013.09.014 (2014).
37 Doi, M. *et al.* Circadian regulation of intracellular G-protein signalling mediates intercellular synchrony and rhythmicity in the suprachiasmatic nucleus. *Nat. Commun.* **2**, 327, doi:10.1038/ncomms1316 (2011).
38 Nakagawa, S., Nguyen Pham, K. T., Shao, X. & Doi, M. Time-Restricted G-Protein Signaling Pathways via GPR176, G(z), and RGS16 Set the Pace of the Master Circadian Clock in the Suprachiasmatic Nucleus. *Int J Mol Sci* **21**, doi:10.3390/ijms21145055 (2020).
39 Wang, T. *et al.* Identification and functional characterisation of N-linked glycosylation of the orphan G protein-coupled receptor Gpr176. *Sci Rep* **10**, 4429, doi:10.1038/s41598-020-61370-y (2020).
40 Hu, Y. *et al.* GWAS of 89,283 individuals identifies genetic variants associated with self-reporting of being a morning person. *Nat Commun* **7**, 10448, doi:10.1038/ncomms10448 (2016).

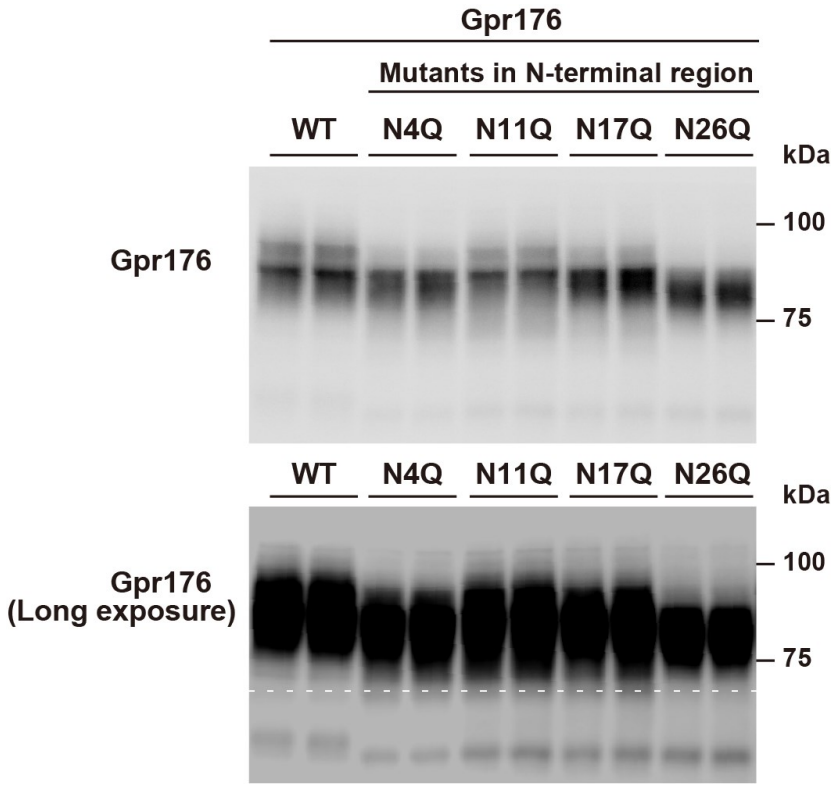

Supplementary Fig. 1 | Comparison of SDS-PAGE migration profiles of WT Gpr176 and mutants containing a single Asn (N) to Gln (Q) substitution of the potential N-terminal glycosylation sites. The WT Gpr176 and respective N4Q, N11Q, N17Q, and N26Q mutants were separately expressed in Flp-In TREx293 cells and subjected to SDS-PAGE/immunoblot analysis with anti-Gpr176 antibody. A longer exposure of the same immunoblot is shown in lower panel. A dashed white horizontal line is overlaid on the high exposure images to emphasize the differences in size between WT and mutants. The WT Gpr176 was recognized as a broad band with a molecular weight slightly higher than 75 kDa. The broadness of the band implies *N*-linked glycosylation heterogeneity. All tested mutants exhibited a small but noticeable change in mobility, with N4Q and N26Q evoking larger mobility changes than N11Q and N17Q. These results suggest that all four N-terminal consensus sites under *N*-glycosylation.

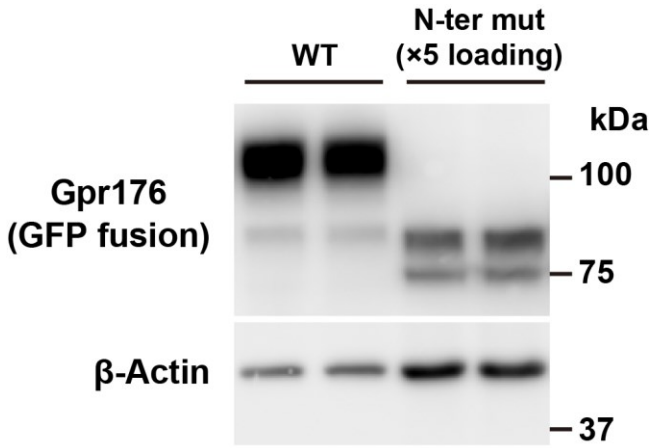

Supplementary Fig. 2 (related to Fig. 3) | *N*-glycosylation deficiency leads to decreased expression of GFP-fused Gpr176. Flp-In TREx293 cells expressing either WT or N-ter mut Gpr176-GFP fusion protein were immunoblotted for Gpr176 (upper) and β-actin (lower). The protein extracts from N-ter mut cells were loaded five-fold over WT cells to increase the sensitivity of protein detection.

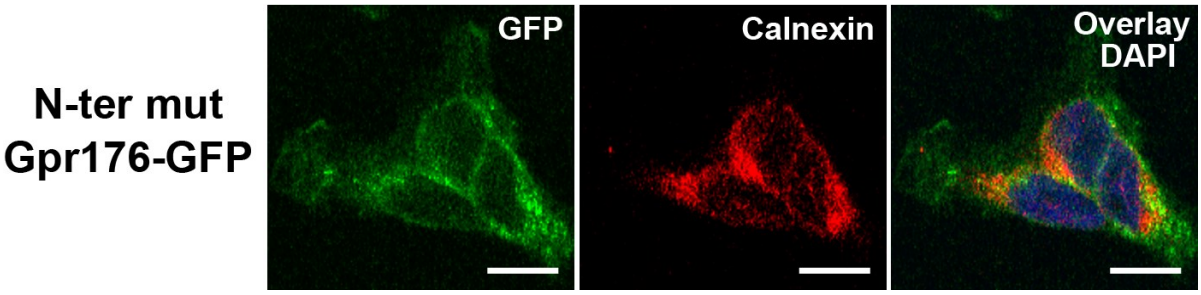

Supplementary Figure 3 (related to Fig. 3) | Partially overlapped localization of N-ter mut Gpr176 and calnexin in Flp-In TREx293 cells. Cells expressing N-ter mut Gpr176-GFP (green) were immunolabeled for calnexin (red). Calnexin is an ER-resident lectin chaperone that binds with N-linked oligosaccharides containing terminal glucose residues. Merged image is a combined image of GFP and calnexin with DAPI (blue). Cells are representative of a population with independent experiments. Scale bars, 10 μm. Note that in the ER, calnexin (red) and N-ter mut Gpr176 (green) were not completely overlapped, likely consistent with the idea that N-ter mutation of Gpr176 results in the loss of N-glycans to which calnexin binds.

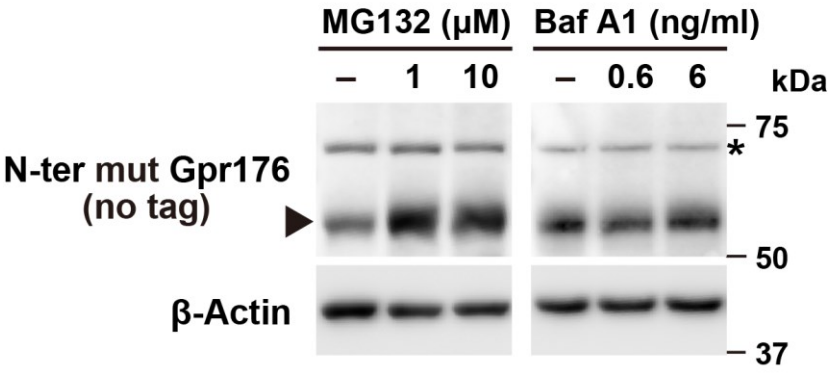

Supplementary Fig. 4 (related to Fig. 3) | Increased level of glycosylation-deficient Gpr176 by treatment with MG132 but not with bafilomycin A1. In this assay, I analyzed non-tagged Gpr176 (i.e., no C-terminal GFP). Flp-In TREx293 cells that express *N*-glycosylation deficient Gpr176 (i.e., N-ter mut) were treated with either MG132 or bafilomycin A1 at the indicated concentrations for 6 hours and immunoblotted for Gpr176 (upper) and β-Actin (lower). Arrowhead indicates the position of non-glycosylated Gpr176. Asterisk, a non-specific band (see **Fig. 2B**).

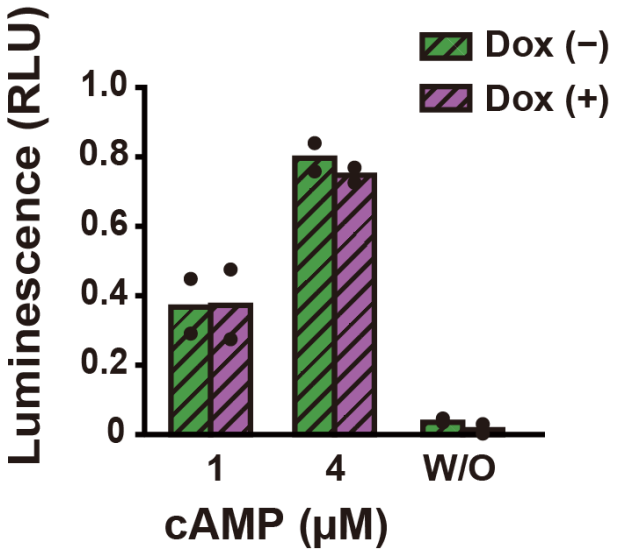

Supplementary Fig. 5 (related to Fig. 4) | Comparable basal GloSensor levels between Dox-treated (+) and untreated (−) cells. The GloSensor system relies on the biosensor expression. To be sure that the intracellular functional GloSensor level does not differ between Dox-treated and non-treated cells, I verified whether their cell lysates are able to show similar GloSensor activities when incubated in vitro with fixed amounts of cAMP. The cells were lysed with or without (w/o) standard cAMP (final conc.: 1 or 4 μM) in buffer containing D-luciferin, Mg^{2+}, and ATP. Luminometry showed that both cell lysates exhibit equivalent dose-dependent GloSensor activities, providing evidence that Dox treatment does not affect GloSensor expression in the cell. Data shown are biological replicates (n = 2, for each condition).

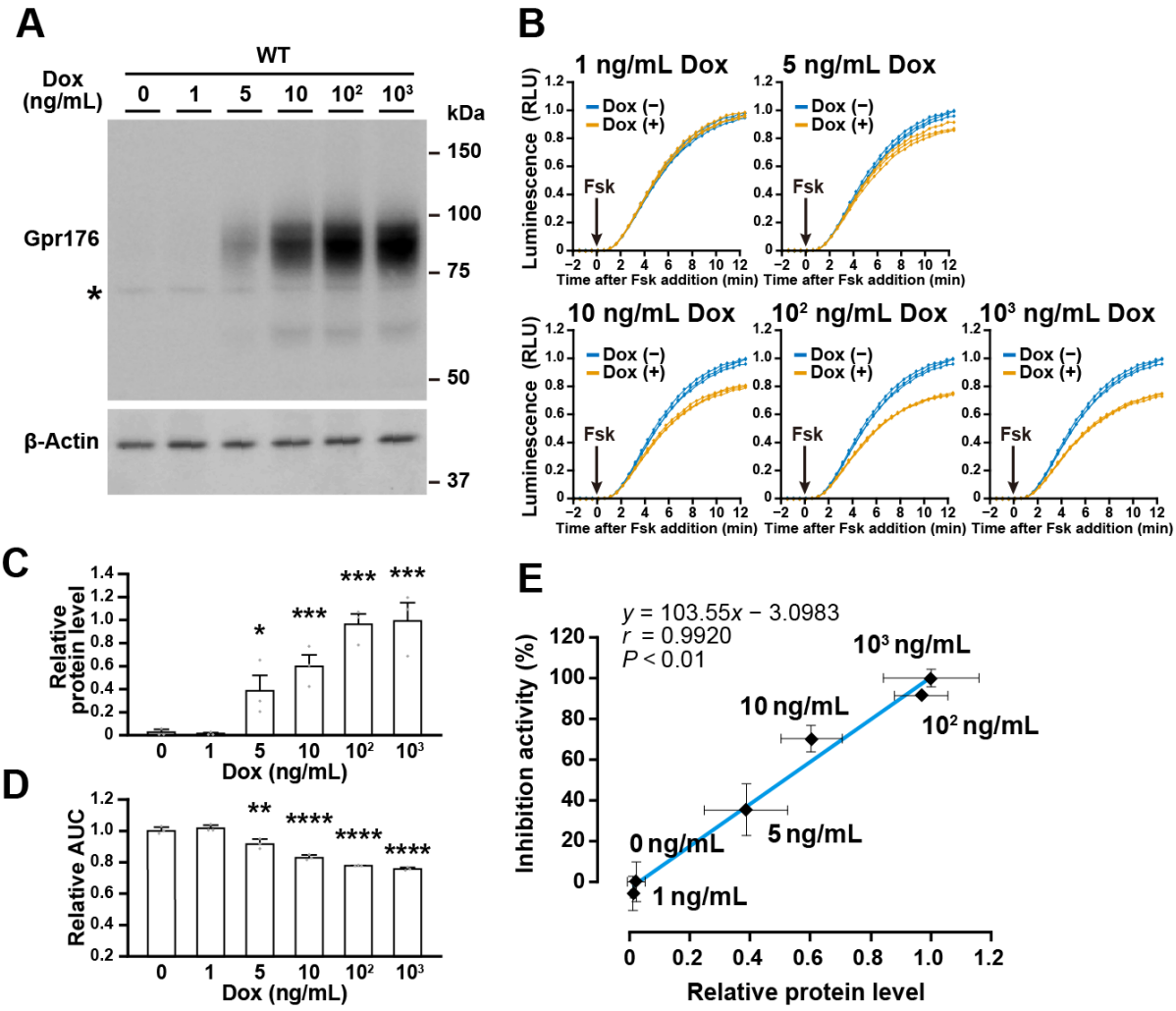

Supplementary Fig. 6 (related to Fig. 4) | Correlation between Gpr176 protein expression level and its cellular cAMP-repressing activity. (**A**) Immunoblot of Flp-In TREx293-Gpr176 (tet-on) cells. Cells were treated with increasing doses of Dox (0. 1, 5, 10, 10^2, and 10^3 ng ml^{-1}) and immunoblotted for Gpr176 (upper) and β-actin (lower). Asterisk, nonspecific bands. (**B**) GloSensor activity traces of Flp-In TREx293-Gpr176 (tet-on) cells. Cells were treated with increasing doses of Dox (0. 1, 5, 10, 10^2, and 10^3 ng/mL). For comparison, GloSensor traces of Dox untreated cells (i.e., 0 ng ml^{-1}) are displayed in parallel. Data represent three independent biological replicates per condition. RLU, relative light units. (**C**) Relative protein levels of Gpr176 dependent on Dox doses. Values are the means ± s.d. ($n = 3$ for each) of the relative band intensities in (**A**). *$P <$ 0.05, ***$P < 0.005$, versus Dox-untreated cells, one-way ANOVA with Bonferroni *post hoc* test. (**D**) Relative area under the curve (AUC) of luminescence values in (**B**). Light emissions were integrated and normalized with those of the untreated control. **$P <$ 0.001, ****$P <$ 0.0001, versus Dox-untreated cells, one-way ANOVA with Bonferroni *post hoc* test. ($n = 3$ for each condition). Error bars indicate s.d. (**E**) Relationship between protein expression level (x axis) and inhibition activity (y axis) of Gpr176 in cells treated with different doses of Dox. Values are the means ± s.d. ($n = 3$ for each). Correlation coefficient (r) and P value were calculated by Pearson product moment correlation coefficient analysis ($r = 0.9920$, $P<0.01$). The linear regression equation is shown at the top of figure.

Chapter 2
Identification of regulation of Gpr176 activity via phosphorylation by T-207219 and other non-orphan GPCRs

Gpr176 is an SCN-enriched orphan receptor that is able to set the pace of circadian behavioural activity rhythm. Therefore, this orphan receptor may be a promising therapeutic target for circadian disorders such as insomnia and lifestyle-related diseases. However, biochemical features that control the activity of Gpr176 are still largely unknown. In **Chapter 1**, I showed that Gpr176 undergoes *N*-glycosylation, which is required for proper cell-surface expression of Gpr176. However, *N*-glycosylation itself is dispensable for Gpr176 to keep its basal (constitutive) activity. In this chapter, using a high-throughput chemical library screening, I identified T-207219 as a modulator for Gpr176 basal activity.

Phosphorylation is a key regulatory post-translational modification described for GPCRs. However, much less is known about phosphorylation and its potential function(s) in orphan GPCRs. I found that T-207219 can induce phosphorylation at two separate conserved serine residues in the C-terminal region of Gpr176, causing receptor internalization. Moreover, using a receptor co-expression system, I obtained evidence that ligand-mediated activation of non-orphan GPCRs leads to phosphorylation of the same residues in Gpr176. Induced phosphorylation, importantly, caused reduced cell-surface expression and second messenger signaling of Gpr176. My data therefore identified a previously uncharacterised inter-GPCRs mechanism in which the orphan receptor is regulated by non-orphan receptors through phosphorylation.

ACKNOWLEDGEMENTS

First and foremost, I would like to express my sincere gratitude to Prof. Masao Doi and Prof. Hitoshi Okamura for accepting me as a member of their laboratory and giving me the opportunity to meet many wonderful people in this world of chronobiology.

In particular, I am deeply grateful to my direct supervisor, Prof. Masao Doi, for his patient guidance, warm encouragement, valuable discussions, and all kinds of advice in research and life. Under Prof. Doi 's instruction, I have learned how to work independently, think logically and solve difficulties in my research. I would not have been able to complete my Ph.D. course without his continuous efforts.

I would like to extend my sincere thanks to Associate prof. Akira Hirasawa from the Department of Genomic Drug Discovery Science for his insightful comments in cell line preparation and Associate prof. Naoyuki Sugiyama from Laboratory of Molecular Systems BioAnalysis for his suggestions and technical assistance in mass spectrometry.

I am grateful to all the members of Doi's lab for their help in life and experiments, which are lovely memories that I treasure. I would like to especially thank Dr. Iori Murai, Dr. Yukari Takahashi, Mr. Genzui Setsu, Mr. Shumpei Nakagawa, Mr. Kaoru Goto and Ms. Kaho Tanaka for their technical contributions in this study.

I would like to thank the Monbukagakusho Honors Scholarship, the AEON Scholarship, the Kyoto University Doctoral Program (KSPD), the Fujitajinsei Scholarship generously established by Prof. Emeritus Tetsuro Fujita and his family, and the Japan Society for the Promotion of Science for financial support during my 10 years of study in Japan. I also thank the Kyoto International Community for helping me with general advice on living in Japan.

To my dearest friends, Dianhui Wei, Shuheng Yan, Yalin Zhang, Chunmei Zou, Jiachen Wang, and Yue Song, your companies made me alive.

Last but not least, I would like to express my gratitude to my parents for their unselfish love and continuous support during my doctoral study and my life in general. Writing this paper is the hardest thing I have ever encountered, and I cannot overcome this without them. Thank for raising me and giving me the strength to go forward fearlessly.